Allyl Isothiocyanate Inhibits Invasion and Angiogenesis in Breast Cancer via EGFR Mediated JAK1/STAT3 Signaling Pathway

Thangarasu Rajakumar
Annamalai University
Pachaiappan Pugalendhi (pugalau@gmail.com)
Annamalai University

Research Article

Keywords: 7,12-dimethylbenz(a)anthracene, JAK-1, STAT-3, angiogenesis, invasion, Allyl isothiocyanate

Posted Date: October 29th, 2021

DOI: https://doi.org/10.21203/rs.3.rs-945897/v1

Abstract

Angiogenesis, invasion, and metastasis are the main events of cancer cells. JAK1/STAT3 is a key intracellular signaling transduction path, which controls the growth, differentiation, apoptosis, invasion, and angiogenesis in various cancer cells. The existing study explored the impact of AITC on the JAK-1/STAT-3 pathway in DMBAinjected rat mammary tumorigenesis. The mammary tumor was initiated through a single dose of 25 mg DMBA/rat through a subcutaneous injection administered near the mammary gland. We observed decreased body weight and augmented the total number of tumors, tumor incidence, tumor volume, well-developed tumor, and histopathological abnormalities in DMBA-injected rats and that were modulated after being treated with AITC. Staining of mammary tissues showed a high accumulation of collagen in DMBAtreated rats and it was normalized by the AITC treatment. Moreover, DMBA-induced mammary tissues showed up-regulated expressions of EGFR, pJAK-1, pSTAT-3, the nuclear fraction of STAT-3, and its associated products like VEGF, VEGFR2, HIF-1α, MMP-2, and MMP-9 and the down-regulated expressions of cytosolic STAT-3 and TIMP-2. Oral administration of AITC on DMBAtreated rats inhibits angiogenesis and invasion through modified these angiogenic and invasive markers. The finding of the current study is further confirmed by molecular docking analysis that shows a strong binding interaction between AITC with STAT-3 and cocrystal structure of STAT3 glide energy of -18.123 and − 72.246 (kcal/mole), respectively. Overall, the results suggested that AITC inhibits activation of the JAK-1/STAT-3 path, which subsequently prevents angiogenesis and invasion. It was recommended that AITC might develop a beneficial effect against breast cancer.

Introduction

Epidermal growth factor (EGF) is a polypeptide that has a mitogenic property. EGF performs via epidermal growth factor receptor (EGFR) and affects cell proliferation-inducing by mammary cells. EGFR is the main target for developing anti-tumor agents, which catalyze the transfer of phosphate molecules from ATP to an active form of tyrosine kinase to trigger a cascade of molecular mechanisms that inhibit cell apoptosis, enhance invasion, and promote angiogenesis responses (Yarden and Sliwkowski, 2001). Activation of EGFR promotes the downstream signal transduction pathway, including the JAK/STAT (Krasinskas, 2011; Ciardiello and Tortora, 2001). JAK-1/STAT-3 is an important intracellular signal transduction pathway in mammary cancer that controls cell growth, invasion, differentiation, apoptosis, and angiogenesis. In response to cytokines (IL-5 and IL-6) and growth factors (interferons and EGF), STAT-3 is phosphorylated by receptors of JAK to form a dimer and translocated into the cell nucleus and it stimulates the expression of genes responsible for cell proliferation, angiogenesis, and invasion (Banerjee and Resat, 2016; Zhang et al. 2003).

Tumor angiogenesis is the formation of new blood vessels that are essential for tumor development and progression (Darakhshan et al. 2013). In the progression stage, malignant cells in primary tumors acquire the ability to penetrate neighboring tissues (invasion) and further enter into lymphatic and blood circulation (metastasis) anchored in different sites to form secondary tumors. Hence, cancer cells escape

lls and remodel their cell-matrix and cell-cell

adhesion molecule to gain invasive and metastatic capabilities (Pecorino, 2012). HIF-1α is considered an important factor that is activated in hypoxic conditions and up-regulates various angiogenesis-related genes, such as VEGF and its receptors like VEGFR2 (Pugh and Ratcliffe, 2003). MMP-2 enzyme plays a vital function in the invasion of tissue basement membranes (Jezierska and Motyl, 2009). MMP-9 is another zinc-dependent peptidase that is activated upon cleavage by various kinds of extracellular proteases (Klein and Bischoff, 2011). TIMP-2 inhibits angiogenesis, endothelial cell proliferation, and migration via MMPdependent and independent-mediated endothelial cells (Bourboulia et al. 2011). The TIMP-2 expression is related to low cancer progression/recurrence or with a poor diagnosis confirming the triggering or the suppressive role of TIMP-2 (Têtu et al. 2006).

The functions of JAK-1/STAT-3 are essential targets for treatment approaches in cancer progression. Natural dietary ingredients and phytochemicals are potential sources of JAK1/STAT-3 inhibitors. Many studies have concluded that intake of fruits and vegetables can reduce cancer incidence (Wang et al. 2016; Shuai and Liu, 2003; Kisseleva et al. 2002). Allyl isothiocyanate (AITC) is a phytochemical present in several dietary sources having various pharmacological properties (Zhang, 2010). Previously, we have reported the anti-oxidative, anti-inflammatory, and anti-cell proliferative properties of AITC in DMBAinjected rat mammary carcinoma through chemopreventive effects (Rajakumar et al. 2015; Rajakumar et al. 2018a, 2018b, 2018c; Thangarasu et al. 2020). However, the action of AITC on the JAK/STAT signaling pathway of mammary cancer is still unclear. Hence, the current work explores the impact of AITC on the JAK-1/STAT-3 pathway for the inhibition of angiogenesis and invasion in DMBAinjected mammary tumorigenesis in rats.

Materials And Methods

Chemicals

AITC and DMBA were obtained from Sigma-Aldrich Chemicals Pvt. Ltd., Bangalore, India. Primary antibodies for EGFR, JAK-1, pJAK-1, STAT-3, pSTAT-3, HIF-1α, VEGF, VEGFR2, MMP-2, MMP-9, TIMP-2, and β-actin were acquired from Santa Cruz Biotechnology, Santa Cruz, CA. All additional chemicals were used by following the analytical standard.

Animals

Female SD rats (6 to 7 weeks of age) were acquired from the NIN, Hyderabad, India. Ethical clearance was granted by the IAEC for the CPCSEA (approval no: 983) guidelines. The rats were kept in Central Animal House, RMMCH, Annamalai University, Chidambaram, Tamilnadu, India. The rats were acclimatized in standard environments of humidity (50±10%), 12 h light/dark cycle, and temperature (24±2˚C). Feed and water were provided *ad libitum*.

40 rats were allocated into four groups of 10 rats in each group. The first group of rats served as untreated controls. Group II and Group III rats have injected a single subcutaneous dose of DMBA (25 mg/rat) near the mammary gland after completion of the first week. Group II rats received no additional treatment. Group III rats received oral administration of AITC (20 mg/kg bwt) through intubation once a day. It began one week before carcinogen exposure and it continued until the completion of the investigation (16 weeks). Group IV rats were administered AITC (20 mg/kg bwt) orally for 16 weeks. Initial and final body weight (bwt) of control and experimental rats were measured during the investigational period. At the end of the 16th week, rats were taken the picture for morphological changes and sacrificed by cervical decapitation. The mammary tumor was removed and tumor volume was measured by using the formula V = 4/3π (D1/2) (D2/2) (D3/2), where D1, D2, and D3 are the three diameters (in mm) of the tumor. Subsequently, mammary tissue was preserved in 10% formalin and stored at -80˚C for histopathological studies.

Histopathological analysis

Mammary tissue was removed and immersed in 10% formalin, dehydrated with 50%-100% ethanol solutions, and embedded in paraffin. Then, paraffinfixed mammary tissue sections (3–5 μm) were cut using a microtome, rehydrated using xylene and graded series of ethanol, and stained with hematoxylin and eosin (H&E). Deposition of collagen was detected by Masson's tri-chrome (MT) and Picrosirius red (PR) staining methods. Images were taken using a Nikon Coolpix 4500 camera, fitted with a microscope of 40× magnification. The deposition of mammary tissue collagen was quantified by standard quantification software ImageJ.

Reverse transcription-polymerase chain reaction analysis

The whole RNA was isolated from the mammary tissues with Trizol reagent approving the Chomczynski and Sacchi (1987) method. The whole RNA was prepared without protein and DNA contamination and quantified spectrophotometrically by determining the absorbance at 260 nm. The reverse transcription (RT) and polymerase chain reaction (PCR) kits were obtained from Invitrogen. The cleansed RNA was reverse transcribed into a single-strand cDNA by using the reverse transcriptase enzyme. The cDNA was amplified with relevant primers of EGFR, JAK-1, STAT-3, HIF-1α, VEGF, VEGFR2, MMP-2, MMP-9, and TIMP-2, as mentioned in Table 1. RT-PCR was conducted under the following conditions: initial denaturation at 95˚C for 2 min, followed by 40 cycles of cyclic denaturation at 94˚C for 15s, annealing at 59˚C for 1 min and extension at 72˚C for 15 sec. GAPDH was used as an internal standard. The amplified PCR products were evaluated by electrophoresis in 2% agarose gels and visualized under UV illumination using ethidium bromide (EtBr)

Table 1
Oligonucleotide primers for RT-PCR.

S.No	Gene name	Forward primer	Reverse primer
1	EGFR	5'-TAACAAGCTCACGCAGTTGG-3'	5'-GTTGAGGGCAATGAGGACAT-3'
2	JAK-1	5'-ATCGCCTCTGATGTCTGGTCTTT-3'	5'-ATCAGGACAGTTGGGTGGAC-3'
3	STAT-3	5'-GGTTGGACATGATGCACACTAT-3'	5'-AGGGCAGACTCAAGTTTATCAG-3'
4	HIF-α	5’-TGCTAATGCCACCACTACC-3’	5’-TGACTCCTTTTCCTGCTCTG-3’
5	VEGF	5’-CTTTCTGCTGTCTTGGGTG-3’	5’-ACTTCGTGATGATTCTGCC-3’
6	VEGFR2	5’-ACGAGGAGAGAGGGTCATCT-3’	5’-GACACACTCTCCTGCTCAGT-3’
7	MMP-2	5’-GCCCTGTCACTCCTGAGAT-3’	5’-GCATCCAGGTTATCGGGGA-3’
8	MMP-9	5’-GTTTGGTGTCGCGGAGCAC-3’	5’-ACATGAGCGCTTCCGGCAC-3’
9	TIMP-2	5'-GTTTTGCAATGCAGACGTAG-3'	5'-ATGTCAAGAAACTCCTGCTT-3'
10	GAPDH	5’-TTCTTGTGCAGTGCCAGCCTCGTC-3’	5’-TAGGAACACGGAAGGCCATGCCAG-3’

Western blotting investigation

Mammary tissue was homogenized with chilled RIPA buffer and centrifuged (12,000 rpm) at 4˚C for 15 min. The supernatant was removed from a tissue homogenate and the concentration of protein was quantified by using the method of Lowry et al. (1951). 50 µg of the total protein samples were separated through 10% SDS-PAGE and transferred onto a PVDF membrane. The membrane was then kept with blocking buffer (5% BSA) for 2 hrs and incubated overnight with specific primary antibodies for EGFR, JAK-1, pJAK-1, STAT-3, pSTAT-3, HIF-1α, VEGF, VEGFR2, MMP-2, MMP-9, TIMP-2, and β-actin at 4˚C. The membrane was thrice cleansed with TBST and kept with its relevant secondary antibodies for 2 hrs at RT. Protein bands were thrice washed with TBST and were observed by using the ECL kit method. Bands were scanned via a scanner and quantities were determined by the ImageJ software.

Molecular docking analysis

A molecular docking work was completed with the Schrodinger suite 2014-2. AITC structure was retrieved from PubChem (). The structure of target protein STAT-3 (PDB ID: 1BG1) was retrieved from the protein data bank (). The receptor grid generation and ligand docking were completed by using the Glide Xp docking algorithm.

Statistical examination

The statistical examination was done by using Statistical Package for the Social Sciences (SPSS) - version 16. The values were represented as mean ± SD. One-way ANOVA, followed by the DMRT comparison system was used to compare differences among the variables. Data were considered statistically significant if *p* values were < 0.05.

Results

Effect of AITC on body weight changes in control and experimental rats

Table 2 demonstrates the bwt of control and experimental rats. Initially, there were no substantial ($p < 0.05$) bwt changes observed in control and experimental rats. Finally, we identified, considerably ($p < 0.05$) reduction in the bwt of DMBA-injected cancer-bearing rats when compared with control rats. In contrast, treatment with AITC prevented the substantial ($p < 0.05$) bwt reduction in DMBA-injected cancer-bearing rats. AITC alone group rats exposed growth in their bwt, but no significant ($p < 0.05$) variations when compared with control rats.

Table 2
Effect of AITC on body weight changes in control and experimental rats.

Groups	Initial weight (g)	Final weight (g)
Control	128.10 ± 10.10	159.30 ± 12.00[a]
DMBA	132.50 ± 10.79	108.45 ± 8.21[b]
DMBA + AITC (20 mg/kg bwt)	133.50 ± 10.32	152.10 ± 11.38[a]
AITC (20 mg/kg bwt)	130.65 ± 9.93	157.75 ± 11.91[a]
Values are set as mean ± SD for 10 rats in each group.		
Values not sharing a common superscript differ substantially at $p < 0.05$.		

Effect of AITC on the total number of tumors, tumor incidence, and tumor volume in control and experimental rats

Table 3 shows the total number of tumors, tumor incidence, and tumor volume of control and experimental rats. This study identified increased tumor numbers and 100% tumor incidence in DMBA-

injected rats. AITC administration in DMBA-induced rats significantly ($p < 0.05$) reduced tumor incidence by 20% and tumor numbers. Moreover, this study demonstrated that 21.86 mm of tumor volume was identified in DMBA-treated rats. Oral supplementation of AITC in DMBA-treated rats significantly ($p < 0.05$) reduced the tumor volume to 4.43 mm (Table 3 and Fig. 1B).

Table 3
Effect of AITC on total number of tumors, tumor incidence and tumor volume in control and experimental rats.

Groups	Total number of tumors (n)	Tumor incidence (%)	Tumor volume (mm^3)/rat
Control	(0)/10	0	0
DMBA	(10)/10	100	21.86 ± 1.57^a
DMBA + AITC (20 mg/kg bwt)	(2)/10	20	4.43 ± 0.33^b
AITC (20 mg/kg bwt)	(0)/10	0	0
Tumor volume was measured using the formula $V = 4/3\pi$ (D1/2) (D2/2) (D3/2), where D1, D2 and D3 are the three diameters (in mm) of the tumor; ( ) indicates total number of rats bearing tumors			
Values are set as mean ± SD for 10 rats in each group.			
Values not sharing a common superscript differ substantially at $p < 0.05$.			

Morphological appearance and histopathological changes of experimental rats

Figure 1 (A and C) shows the morphological appearance and histopathological changes of DMBA and DMBA + AITC treated rats. This study was observed a well-developed tumor in DMBA-injected rats, which was reduced with AITC treatment. Additionally, DMBA-injected tumor-bearing rats showed loss of architecture with infiltrating malignant tumors. DMBA + AITC treated rats indicated near-normal architecture of mammary tissues with an increased area of fibrosis.

Effect of AITC on MT and PR staining in mammary tissue

Figure 2 (a-d) shows the pathological investigation of MT and PR staining of mammary tissue for collagen deposition. Collagen was augmented considerably ($p < 0.05$) in DMBAinjected rat mammary tissue and it decreased in DMBA + AITC supplemented rats. Collagen deposition was normal among AITC only administered and normal control rats.

hosphorylation and nuclear translocation

To investigate whether AITC affects the activation of JAK/STAT signaling in DMBA-induced mammary tumors, we analyzed the mRNA and protein expressions of EGFR, pJAK-1, tJAK-1, pSTAT-3, the cytosolic and nuclear fraction of STAT-3 and tSTAT-3 in AITC treated cancer-bearing rats. Our results have shown that DMBA-induced rats significantly ($p < 0.05$) increased the expression of EGFR, pJAK-1, pSTAT-3, and nuclear STAT-3 and decreased expression of cytosolic STAT-3 compared to control rats. Oral administration of AITC inhibited JAK/STAT signaling by decreasing the expression of EGFR, and pJAK-1 and blocking STAT-3 phosphorylation and nuclear translocation compared with DMBAinduced cancer-bearing rats. Moreover, oral supplementation of AITC had no obvious ($p < 0.05$) effect on the mRNA and protein expression of tJAK-1 and tSTAT-3 compared to other groups (Fig. 3). This result suggested that AITC mediated effect on angiogenesis and invasion in mammary cancer involves the inhibition of STAT-3 activation, indicating that AITC might be a better compound in suppressing mammary tumor growth.

AITC blocks angiogenesis formation via inhibiting JAK/STAT pathway

As neovascularization plays a major role in tumor growth and is one of the most important downstream events triggered by the JAK/STAT pathway. To know whether AITC blocks angiogenesis formation via inhibition of the JAK/STAT pathway, we investigated the effect of AITC on angiogenic markers such as HIF-1α, VEGF, and VEGFR2 in DMBA-injected rats. Figure 4 shows the mRNA and protein expressions wherein HIF-1α, VEGF, and VEGFR2 were considerably ($p < 0.05$) augmented in DMBAinjected tumor-bearing rats when evaluated with control rats. Oral administration of AITC significantly ($p < 0.05$) reduced the expression of HIF-1α, VEGF, and VEGFR2 compared to DMBA-injected rats. There were no substantial ($p < 0.05$) alterations observed in the expression of angiogenic markers in AITC only treated and normal control rats. These data suggested that AITC blocked angiogenesis formation in DMBA-induced tumor-bearing rats via prevention of the JAK/STAT signaling pathway.

AITC impedes invasion via inhibiting JAK/STAT pathway

An invasion is a crucial step in the development of tumor metastasis, which includes the secretion of substances that degrade the extracellular matrix (ECM), basement membrane (BM), and up-regulation of protein controlling cell motility and migration. To determine whether inhibition of the JAK/STAT pathway by AITC impedes invasion, we analyzed the expression of invasive markers like MMP-2 and MMP-9 and their inhibitor TIMP-2 in DMBA-induced rats. Figure 5 shows the mRNA and protein expressions wherein MMP-2 and MMP-9 were noticeably ($p < 0.05$) augmented and TIMP-2 was markedly ($p < 0.05$) reduced in DMBA-injected cancer-bearing rats when evaluated with control rats. Oral administration of AITC significantly ($p < 0.05$) modulated the expression of MMP-2, MMP-9, and TIMP-2 compared to DMBA-injected rats. There were no significant ($p < 0.05$) variations identified in the expression of invasive markers in AITC only treated and normal control rats. These findings clearly showed that AITC impeded

AITC binds to STAT-3

To further confirm the inhibition of JAK/STAT signaling by AITC, we next investigated molecular docking studies of the binding interaction of AITC with STAT-3 and the cocrystal structure of STAT-3. Figure 6 (A1 and A2) indicates the molecular docking findings and the data confirmed that AITC reveals a phenomenal binding interaction with STAT-3 and cocrystal structure of STAT-3 with glide energy of 18.123 and 72.246 (kcal/mole), respectively. A1 denotes that AITC forms a hydrogen bond with Gln 326 and hydrophobic interactions with Gln 247, Pro 336, Cys 251, and Ile 258 of STAT-3. A2 denotes that AITC forms a hydrogen bond with Asp 261, Cys 259, Asn 257, Ala 250, and Pro 333, and hydrophobic interactions with Ile 258, Glu 324, Leu 260, Gln 247, Cys 251, Pro 336, Gly 253, Pro 256, and Ser 514 of the cocrystal structures of STAT-3. Based on these glide energy, hydrogen bonds, and hydrophobic interactions, we detected that the AITC might have a better binding affinity with STAT-3 and cocrystal structure of STAT-3 and ultimately inhibited JAK/STAT signaling pathway.

Discussion

Reactive oxygen species (ROS) generation and peroxidation of membrane lipids are related to the initiation and progression of cancer that affecting the normal biochemical mechanism which further leads to the bwt reduction (Davis and Kuttan, 2001). In the present study, the total bwt of DMBA-induced rats was reduced due to the changes in the energy metabolism during tumor formation and development (Moselhy and Al mslmani, 2008). AITC treated rats gradually improved bwt, which specified that the reduced level of ROS formation and lipid peroxidation could be attributed to the free radical scavenging activity of AITC (Rajakumar et al. 2015). AITC efficiently reduced the total number of tumors, tumor incidence and tumor volume in cancer-bearing rats might be due to inhibitory action or anti-tumor activity. The anti-tumor activity of AITC has been reported against various cancer cell lines (Srivastava et al. 2003; Bhattacharya et al. 2012). Kumar et al. (2011) reported that AITC might disrupt the energy requirement of tumor tissue and lead to the suppression of tumor growth.

Histopathological investigation of mammary tissues of cancer-bearing rats indicated carcinomas exhibited infiltrating malignant tumors. On the contrary, AITC treated rats shown no sign of cellular proliferation and necrosis that was proved by the normal architecture of mammary tissue with an increased area of fibrosis. Hence, it proposes that the AITC has the potential to be safe and effective in cancer management and also evidences the anti-neoplastic activity (Rajakumar et al. 2015). Collagen in tissues is a physical barrier against tumor invasion and metastasis (Fang et al. 2014). Collagen around normal epithelial cells in breast tissue is normally curly and smooth. In tumors, collagen gradually thickens, stiffens, and linearizes and it activates metastasis by fostering cell migration into the extracellular matrix (Wyckoff et al. 2007). In the present study, over accumulation of collagen was detected in cancer-bearing rats, which is in agreement with earlier reports of pathological parameters in mammary tissues (Arivazhagan and Sorimuthu Pillai, 2014). On the other hand, oral supplementation of AITC to DMBAtreated rats ameliorated the accumulation of collagen in mammary tissues.

EGFR plays a vital function in the control of cell growth, differentiation, proliferation, survival, and apoptosis during development and homeostasis (Normanno et al. 2006; Jorissen et al. 2003). EGFR homodimers are activated after binding with their ligand (EGF), followed by transphosphorylation of several tyrosine kinase domains, and subsequent activation of STAT proteins (Spano et al. 2005). After activation, STAT-3 undergoes tyrosine phosphorylation, dimerization, DNA binding, and transcriptional activation of genes associated with cell division and survival. The interaction between JAK and STAT-3 mediates the transient phosphorylation of STAT-3 in normal cells, but in most cancer cells, which are constitutively phosphorylated (Leeman-Neill et al. 2009). The cascade effect of STAT-3 includes several molecules, such as HIF-1α and VEGF for angiogenesis and MMP-2 and MMP-9 for invasion (Jarnicki et al. 2010; Aggarwal et al. 2006). Phytochemicals that suppress the activation of STAT-3 have been considered as potential agents for the inhibition and therapy of cancer (Wang et al., 2016). Lai et al. (2014) reported that AITC suppresses the invasion, migration, and metastasis of EGFstimulated MAPK signaling pathways in HT29 cells. Supportive with previous reports, the present study substantiates that AITC treatment abrogates the stimulation of STAT-3 phosphorylation, followed by nuclear translocation. Moreover, interactions of AITC with STAT-3 dimerization site are validated by molecular docking analysis, which strengthens the result. It was found that AITC acts as a ligand for EGFR and it, therefore, inhibits STAT-3 phosphorylation, nuclear translocation, and its cascade activation.

Angiogenesis is a key process for tumor development, invasion, and metastasis, and it is a possible target for cancer treatment (Raica et al. 2009). VEGF is an important survival mediator of vascular endothelial cells, which activate tyrosine kinase that subsequently binds to VEGFR. VEGFR2 is the main factor of VEGF-mediated angiogenesis (Korpanty et al. 2011). Previous studies reported that decreased production of VEGF and VEGFR2 in AITCtreated mice, which indicates the anti-angiogenic effect of AITC in ascites tumor growth (Kumar et al. 2009). In this study, AITC treatment down-regulated VEGF and VEGFR2 expression in cancer-bearing rats, it may be due to its anti-angiogenic potential. HIF-1 is the heterodimeric transcriptional mediator containing α and β sub-units (Yang et al. 2004). HIF-1α overexpression is related to tumor growth, mortality, treatment failure, and vascularity (Kubo et al. 2016). Previous studies reported that sulforaphane, a natural analog of AITC, induced down-regulation of HIF-1α expression in HMEC-1 cells (Bertl et al. 2006). Consistent with earlier reports, our results suggested that AITC suppresses the HIF-1α overexpression in cancer-bearing rats.

In tumor invasion, tumor cells residing within a primary tumor invade the nearby stroma and adjacent normal tissue (Quail and Joyce, 2013). MMP-2, an enzyme that damages ECM components, plays a crucial function in cell migration during pathological and physiological mechanisms (Jezierska and Motyl, 2009). MMP-9 is another enzyme that performs a key function in cancer development, progression, invasion, and metastasis (Duffy et al. 2000). Inhibition of MMP expression or reduced enzyme quantity can be an important process that could serve as an early target for blocking cancer metastasis (Guruvayoorappan and Kuttan, 2008). In the present study, we observed that AITC repressed MMP-9 and MMP-2 at both mRNA and protein expressions in DMBA-induced mammary cancer, which was coinciding with the previous report in human hepatoma SK-Hep1 cells (Hwang and Lee, 2006). TIMP-2 plays a

d TIMP-2 level prevents pro-MMP2 activation

that reduces tumor angiogenesis and invasion (Munshi et al. 2004). Previous studies reported that AITC treatment significantly improved the formation of TIMP and it is a suppressor of the MMP function of HUVECs cells (Thejass and Kuttan, 2007). In the present study, DMBAinjected rats show decreased expression of TIMP-2. It significantly increased upon AITC treatment, which may be due to its anti-invasive potential.

Conclusion

EGFR and its downstream JAK/STAT pathway are possibly key processes in the pathogenesis of breast cancer. These processes have emerged as an effective target for both inhibition and therapeutics of breast cancer. Our work exhibited that AITC inhibits the EGFR mediated JAK1/STAT-3 signaling and downstream molecules associated with angiogenesis and invasion via suppression of STAT-3 phosphorylation, and prevents nuclear translocation of STAT-3 (Fig. 7). This is confirmed through molecular docking analysis of the interaction of AITC with STAT-3 molecule. Thus, AITC might improve the positive effect against breast cancer.

Declarations

Acknowledgment

We gratefully acknowledge the financial assistance from the Indian Council of Medical Research (ICMR, Grant number-3/2/2/189/2013/NCD-III (OPA-27129)), in the form of Senior Research Fellowship (SRF), New Delhi, India to the first author, Mr. T. Rajakumar.

Conflict of interest

The author declares that there are no conflicts of interest.

ORCID iD

Dr. T. Rajakumar, https://orcid.org/0000-0003-1168-8464

Dr. P. Pugalendhi, https://orcid.org/0000-0003-0811-1533

References

1. Aggarwal BB, Sethi G, Ahn KS, Sandur SK, Pandey MK, Kunnumakkara AB, Sung B, Ichikawa H (2006) Targeting signal-transducer-and-activator-of-transcription-3 for prevention and therapy of cancer: modern target but ancient solution. Ann N Y Acad Sci 1091:151–169

2. Arivazhagan L, Sorimuthu Pillai S (2014) Tangeretin, a citrus pentamethoxyflavone, exerts cytostatic effect via p53/p21 up-regulation and suppresses metastasis in 7,12-dimethylbenz(α)anthracene-induced rat mammary carcinoma. J Nutr Biochem 25:1140–1153
3. Banerjee K, Resat H (2016) Constitutive activation of STAT3 in breast cancer cells: A review. Int J Cancer 138:2570–2578
4. Bertl E, Bartsch H, Gerhäuser C (2006) Inhibition of angiogenesis and endothelial cell functions are novel sulforaphane-mediated mechanisms in chemoprevention. Mol Cancer Ther 5:575–585
5. Bhattacharya A, Li Y, Geng F, Munday R, Zhang Y (2012) The principal urinary metabolite of allyl isothiocyanate, N-acetyl-S-(N-allylthiocarbamoyl)cysteine, inhibits the growth and muscle invasion of bladder cancer. Carcinogenesis 33:394–398
6. Bourboulia D, Jensen-Taubman S, Rittler MR, Han HY, Chatterjee T, Wei B, Stetler-Stevenson WG (2011) Endogenous angiogenesis inhibitor blocks tumor growth via direct and indirect effects on tumor microenvironment. Am J Pathol 179:2589–2600
7. Chomczynski P, Sacchi N (1987) Single-step method of RNA isolation by acid guanidinium thiocyanate-phenol-chloroform extraction. Anal Biochem 162:156–159
8. Ciardiello F, Tortora G (2001) A novel approach in the treatment of cancer: targeting the epidermal growth factor receptor. Clin Cancer Res 7:2958–2970
9. Darakhshan S, Bidmeshkipour A, Khazaei M, Rabzia A, Ghanbari A (2013) Synergistic effects of tamoxifen and tranilast on VEGF and MMP-9 regulation in cultured human breast cancer cells. Asian Pac J Cancer Prev 14:6869–6874
10. Davis L, Kuttan G (2001) Effect of Withania somnifera on DMBA induced carcinogenesis. J Ethnopharmacol 75:165–168
11. Duffy MJ, Maguire TM, Hill A, McDermott E, O'Higgins N (2000) Metalloproteinases: role in breast carcinogenesis, invasion and metastasis. Breast Cancer Res 2:252–257
12. Fang M, Yuan J, Peng C, Li Y (2014) Collagen as a double-edged sword in tumor progression. Tumour Biol 35:2871–2882
13. Guruvayoorappan C, Kuttan G (2008) Amentoflavone inhibits experimental tumor metastasis through a regulatory mechanism involving MMP-2, MMP-9, prolyl hydroxylase, lysyl oxidase, VEGF, ERK-1, ERK-2, STAT-1, NM23 and cytokines in lung tissues of C57BL/6 mice. Immunopharmacol Immunotoxicol 30:711–727
14. Hwang ES, Lee HJ (2006) Allyl isothiocyanate and its N-acetylcysteine conjugate suppress metastasis via inhibition of invasion, migration, and matrix metalloproteinase-2/-9 activities in SK-Hep 1 human hepatoma cells. Exp Biol Med (Maywood) 231:421–430
15. Jarnicki A, Putoczki T, Ernst M (2010) Stat3: linking inflammation to epithelial cancer - more than a "gut". feeling? Cell Div 5:14
16. Jezierska A, Motyl T (2009) Matrix metalloproteinase-2 involvement in breast cancer progression: a mini-review. Med Sci Monit 15:RA32–R40

17. Jorissen RN, Walker F, Pouliot N, Garrett TP, Ward CW, Burgess AW (2003) Epidermal growth factor receptor: mechanisms of activation and signalling. Exp Cell Res 284:31–53
18. Kisseleva T, Bhattacharya S, Braunstein J, Schindler CW (2002) Signaling through the JAK/STAT pathway, recent advances and future challenges. Gene 285:1–24
19. Klein T, Bischoff R (2011) Physiology and pathophysiology of matrix metalloproteases. Amino Acids 41:271–290
20. Korpanty G, Smyth E, Carney DN (2011) Update on anti-angiogenic therapy in non-small cell lung cancer: Are we making progress? J Thorac Dis 3:19–29
21. Krasinskas AM (2011) EGFR Signaling in Colorectal Carcinoma. Patholog Res Int 2011:932932
22. Kubo H, Kitajima Y, Kai K, Nakamura J, Miyake S, Yanagihara K, Morito K, Tanaka T, Shida M, Noshiro H (2016) Regulation and clinical significance of the hypoxia-induced expression of ANGPTL4 in gastric cancer. Oncol Lett 11:1026–1034
23. Kumar A, D'Souza SS, Tickoo S, Salimath BP, Singh HB (2009) Antiangiogenic and proapoptotic activities of allyl isothiocyanate inhibit ascites tumor growth in vivo. Integr Cancer Ther 8:75–87
24. Kumar GS, Ramakrishnan V, Madhusudhanan N, Balasubramanian MP (2011) Antioxidant activity of Allyl isothiocyanate [AITC] against N-nitrosodiethylamine induced experimental liver carcinogenesis. J Pharm Res 4:3690–3694
25. Lai KC, Lu CC, Tang YJ, Chiang JH, Kuo DH, Chen FA, Chen IL, Yang JS (2014) Allyl isothiocyanate inhibits cell metastasis through suppression of the MAPK pathways in epidermal growth factor–stimulated HT29 human colorectal adenocarcinoma cells. Oncol Rep 31:189–196
26. Leeman-Neill RJ, Wheeler SE, Singh SV, Thomas SM, Seethala RR, Neill DB, Panahandeh MC, Hahm ER, Joyce SC, Sen M, Cai Q, Freilino ML, Li C, Johnson DE, Grandis JR (2009) Guggulsterone enhances head and neck cancer therapies via inhibition of signal transducer and activator of transcription-3. Carcinogenesis 30:1848–1856
27. Lowry OH, Rosebrough NJ, Farr AL, Randall RJ (1951) Protein measurement with the Folin phenol reagent. J Biol Chem 193:265–275
28. Moselhy SS, Al mslmani MA (2008) Chemopreventive effect of lycopene alone or with melatonin against the genesis of oxidative stress and mammary tumors induced by 7,12 dimethyl(a)benzanthracene in sprague dawely female rats. Mol Cell Biochem 319:175–180
29. Munshi HG, Wu YI, Mukhopadhyay S, Ottaviano AJ, Sassano A, Koblinski JE, Platanias LC, Stack MS (2004) Differential regulation of membrane type 1-matrix metalloproteinase activity by ERK 1/2- and p38 MAPK-modulated tissue inhibitor of metalloproteinases 2 expression controls transforming growth factor-beta1-induced pericellular collagenolysis. J Biol Chem 279:39042–39050
30. Normanno N, De Luca A, Bianco C, Strizzi L, Mancino M, Maiello MR, Carotenuto A, De Feo G, Caponigro F, Salomon DS (2006) Epidermal growth factor receptor (EGFR) signaling in cancer. Gene 366:2–16
31. Pecorino L (2012) Molecular biology of cancer: Mechanisms, targets and therapeutics. Oxford

32. Pugh CW, Ratcliffe PJ (2003) Regulation of angiogenesis by hypoxia: role of the HIF system. Nat Med 9:677–684
33. Quail DF, Joyce JA (2013) Microenvironmental regulation of tumor progression and metastasis. Nat Med 19:1423–1437
34. Raica M, Cimpean AM, Ribatti D (2009) Angiogenesis in pre-malignant conditions. Eur J Cancer 45:1924–1934
35. Rajakumar T, Pugalendhi P, Jayaganesh R, Ananthakrishnan D, Gunasekaran K (2018b) Effect of allyl isothiocyanate on NF-κB signaling in 7,12-dimethylbenz(a)anthracene and N-methyl-N-nitrosourea-induced mammary carcinogenesis. Breast Cancer 25:50–59
36. Rajakumar T, Pugalendhi P, Thilagavathi S, Ananthakrishnan D, Gunasekaran K (2018c) Allyl isothiocyanate, a potent chemopreventive agent targets AhR/Nrf2 signaling pathway in chemically induced mammary carcinogenesis. Mol Cell Biochem 437:1–12
37. Rajakumar T, Pugalendhi P, Thilagavathi S (2015) Dose response chemopreventive potential of allyl isothiocyanate against 7,12-dimethylbenz(a)anthracene induced mammary carcinogenesis in female Sprague-Dawley rats. Chem Biol Interact 231:35–43
38. Rajakumar T, Pugalendhi P, Thilagavathi S (2018a) Protective Effect of Allyl Isothiocyanate on Glycoprotein Components in 7,12-dimethylbenz(a)anthracene Induced Mammary Carcinoma in Rats. Indian J Clin Biochem 33:171–177
39. Shuai K, Liu B (2003) Regulation of JAK-STAT signalling in the immune system. Nat Rev Immunol 3:900–911
40. Spano JP, Fagard R, Soria JC, Rixe O, Khayat D, Milano G (2005) Epidermal growth factor receptor signaling in colorectal cancer: preclinical data and therapeutic perspectives. Ann Oncol 16:189–194
41. Srivastava SK, Xiao D, Lew KL, Hershberger P, Kokkinakis DM, Johnson CS, Trump DL, Singh SV (2003) Allyl isothiocyanate, a constituent of cruciferous vegetables, inhibits growth of PC-3 human prostate cancer xenografts in vivo. Carcinogenesis 24:1665–1670
42. Têtu B, Brisson J, Wang CS, Lapointe H, Beaudry G, Blanchette C, Trudel D (2006) The influence of MMP-14, TIMP-2 and MMP-2 expression on breast cancer prognosis. Breast Cancer Res 8:R28
43. Thangarasu R, Pachaiappan P, Subbaiyan T (2020) Anti-Estrogenic and Anti-Cell Proliferative Effect of Allyl Isothiocyanate in Chemoprevention of Chemically Induced Mammary Carcinogenesis in Rats. Pathol Oncol Res 26:913–925
44. Thejass P, Kuttan G (2007) Inhibition of endothelial cell differentiation and proinflammatory cytokine production during angiogenesis by allyl isothiocyanate and phenyl isothiocyanate. Integr Cancer Ther 6:389–399
45. Wang G, Jing Y, Cao L, Gong C, Gong Z, Cao X (2016) A novel synthetic Asiatic acid derivative induces apoptosis and inhibits proliferation and mobility of gastric cancer cells by suppressing STAT3 signaling pathway. Onco Targets Ther 10:55–66
46. Wyckoff JB, Wang Y, Lin EY, Li JF, Goswami S, Stanley ER, Segall JE, Pollard JW, Condeelis J (2007) ell intravasation in mammary tumors. Cancer

Res 67:2649–2656

47. Yang DI, Chen SD, Yang YT, Ju TC, Xu JM, Hsu CY (2004) Carbamoylating chemoresistance induced by cobalt pretreatment in C6 glioma cells: putative roles of hypoxia-inducible factor-1. Br J Pharmacol 141:988–996
48. Yarden Y, Sliwkowski MX (2001) Untangling the ErbB signalling network. Nat Rev Mol Cell Biol 2:127–137
49. Zhang F, Li C, Halfter H, Liu J (2003) Delineating an oncostatin M-activated STAT3 signaling pathway that coordinates the expression of genes involved in cell cycle regulation and extracellular matrix deposition of MCF-7 cells. Oncogene 22:894–905
50. Zhang Y (2010) Allyl isothiocyanate as a cancer chemopreventive phytochemical. Mol Nutr Food Res 54:127–135

Figures

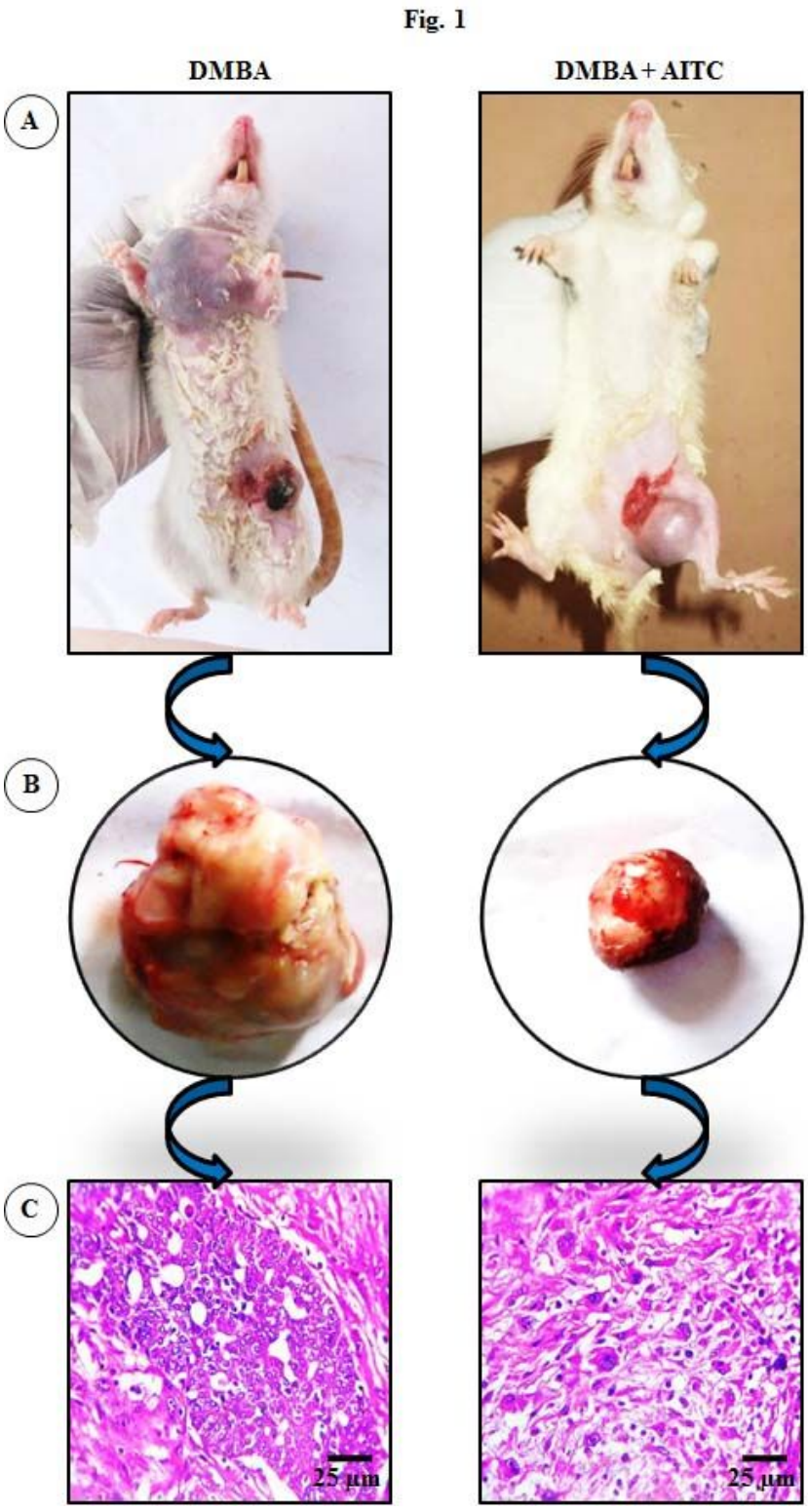

Figure 1

Illustrative images show the gross appearance (A), mammary tumor size (B), and histopathological structures (C) of DMBA and DMBA+AITC treated rats, respectively.

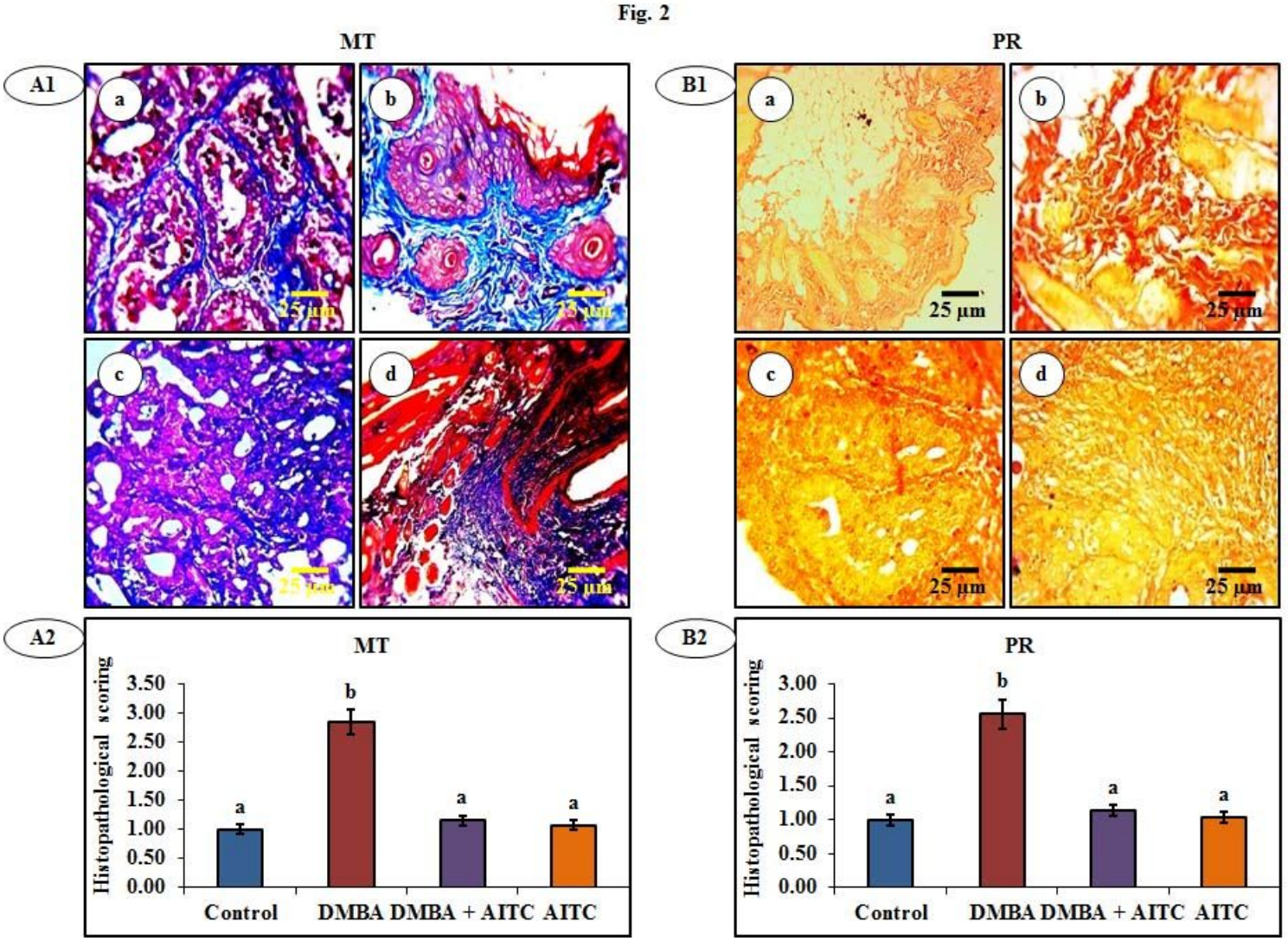

Figure 2

Pathological investigation of MT and PR staining (a-d) in the mammary tissues of control and experimental rats. (A1) Photomicrography image shows the pathological analysis of MT staining. (A2) The representative graph shows the histological scoring of collagen deposition in pathological analysis of MT. (B1) Photomicrography image shows the pathological analysis of PR staining. (B2) The representative graph shows the histological scoring of collagen deposition in pathological analysis of PR. Control (a) and AITC only administered (d) rats indicated normal expression of collagen deposition; DMBA injected (b) rats presented augmented collagen deposition. However, DMBA+AITC treated (c) rats showed decreased collagen deposition in mammary tissues. 40× magnification.

Fig. 3

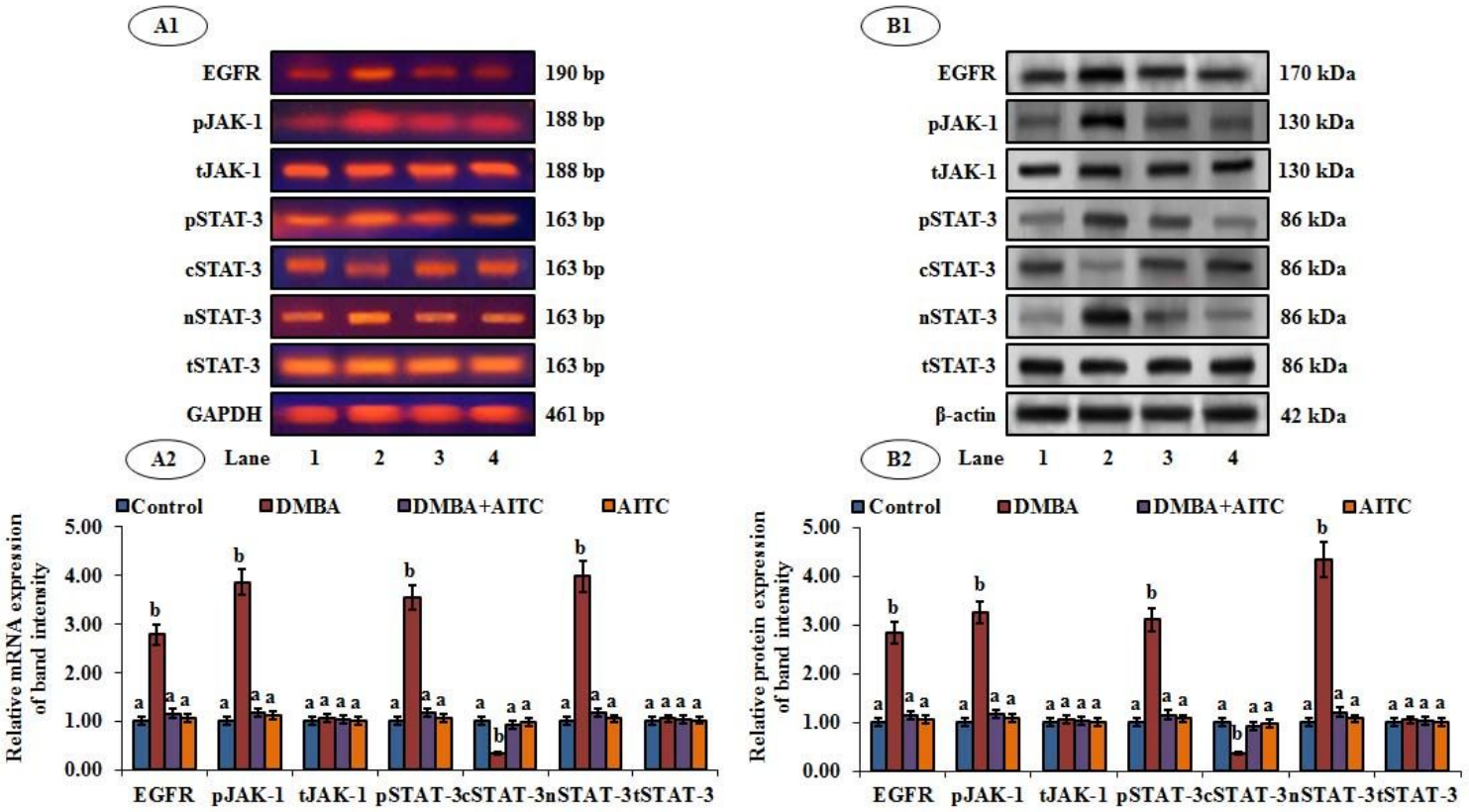

Figure 3

Expressions of EGFR, pJAK-1, tJAK-1, pSTAT-3, cSTAT-3, nSTAT-3 and tSTAT-3 in mammary tissues of control and experimental rats. (A1) Representative RT-PCR analysis shows the band intensity quantified by densitometry and normalized to respective GAPDH loading control. (A2) Representative graph shows the relative mRNA expression of fold changes in RT-PCR. (B1) Representative western blotting analysis shows the band intensity quantified by densitometry and normalized to respective β-actin loading control. (B2) Representative graph shows the relative protein expression of fold changes in western blot. Lane 1: control rats; Lane 2: DMBA injected rats; Lane 3: DMBA with AITC treatment; Lane 4: AITC only administered rats. Values are set as mean ± SD for 10 rats in each group. Values not sharing a common superscript differ substantially at $p<0.05$. Phosphorylated JAK-1 (pJAK-1), total JAK-1 (tJAK-1), phosphorylated STAT-3 (pSTAT-3), cytosolic fraction of STAT-3 (cSTAT-3), nuclear fraction of STAT-3 (nSTAT-3) and total STAT-3 (tJAK-1).

Fig. 4

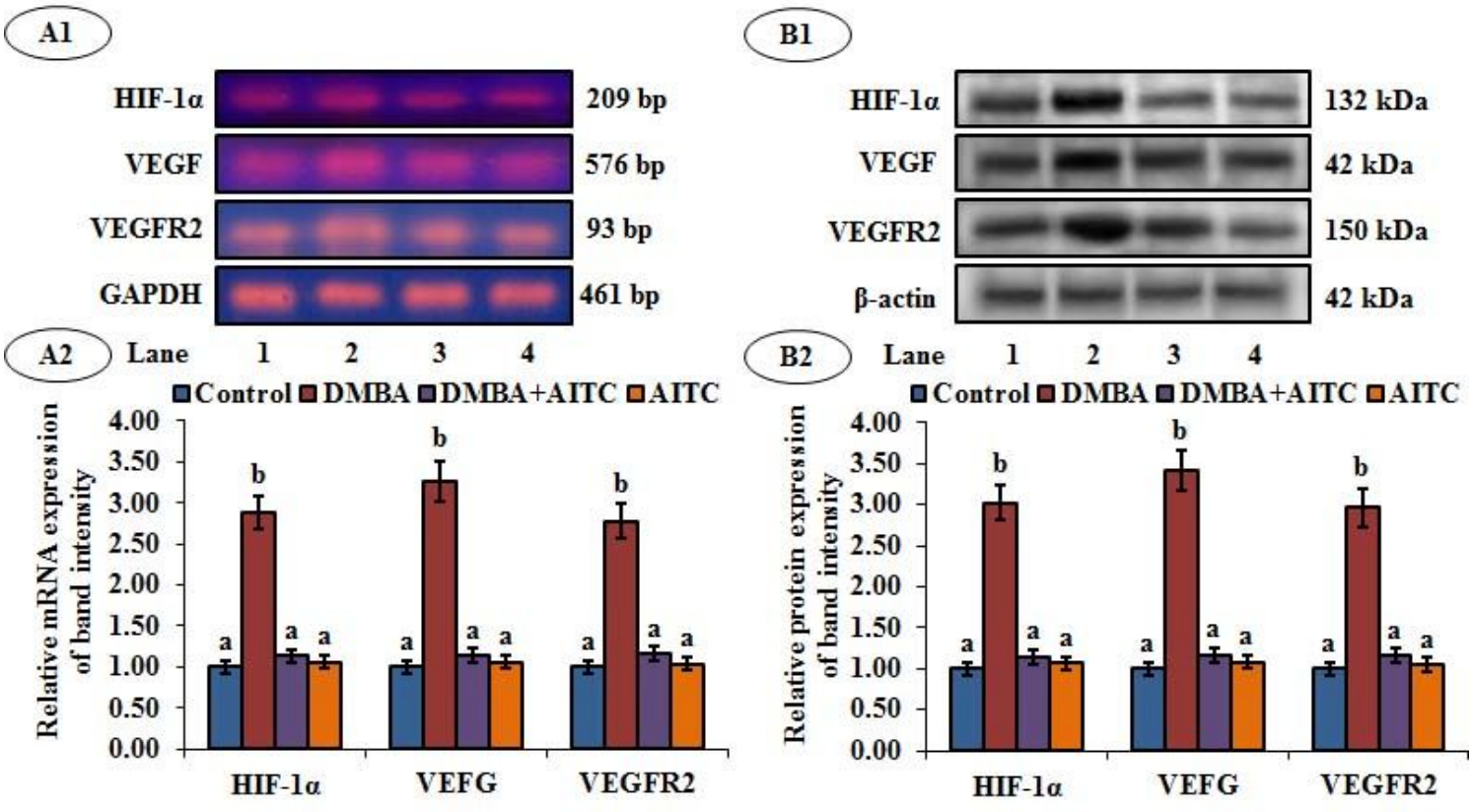

Figure 4

Expressions of HIF-1α, VEGF, and VEGFR2 in mammary tissues of control and experimental rats. (A1) Representative RT-PCR analysis shows the band intensity quantified by densitometry and normalized to respective GAPDH loading control. (A2) Representative graph shows the relative mRNA expression of fold changes in RT-PCR. (B1) Representative western blotting analysis shows the band intensity quantified by densitometry and normalized to respective β-actin loading control. (B2) Representative graph shows the relative protein expression of fold changes in western blot. Lane 1: control rats; Lane 2: DMBA injected rats; Lane 3: DMBA with AITC treatment; Lane 4: AITC only administered rats. Values are set as mean ± SD for 10 rats in each group. Values not sharing a common superscript differ substantially at $p<0.05$.

Fig. 5

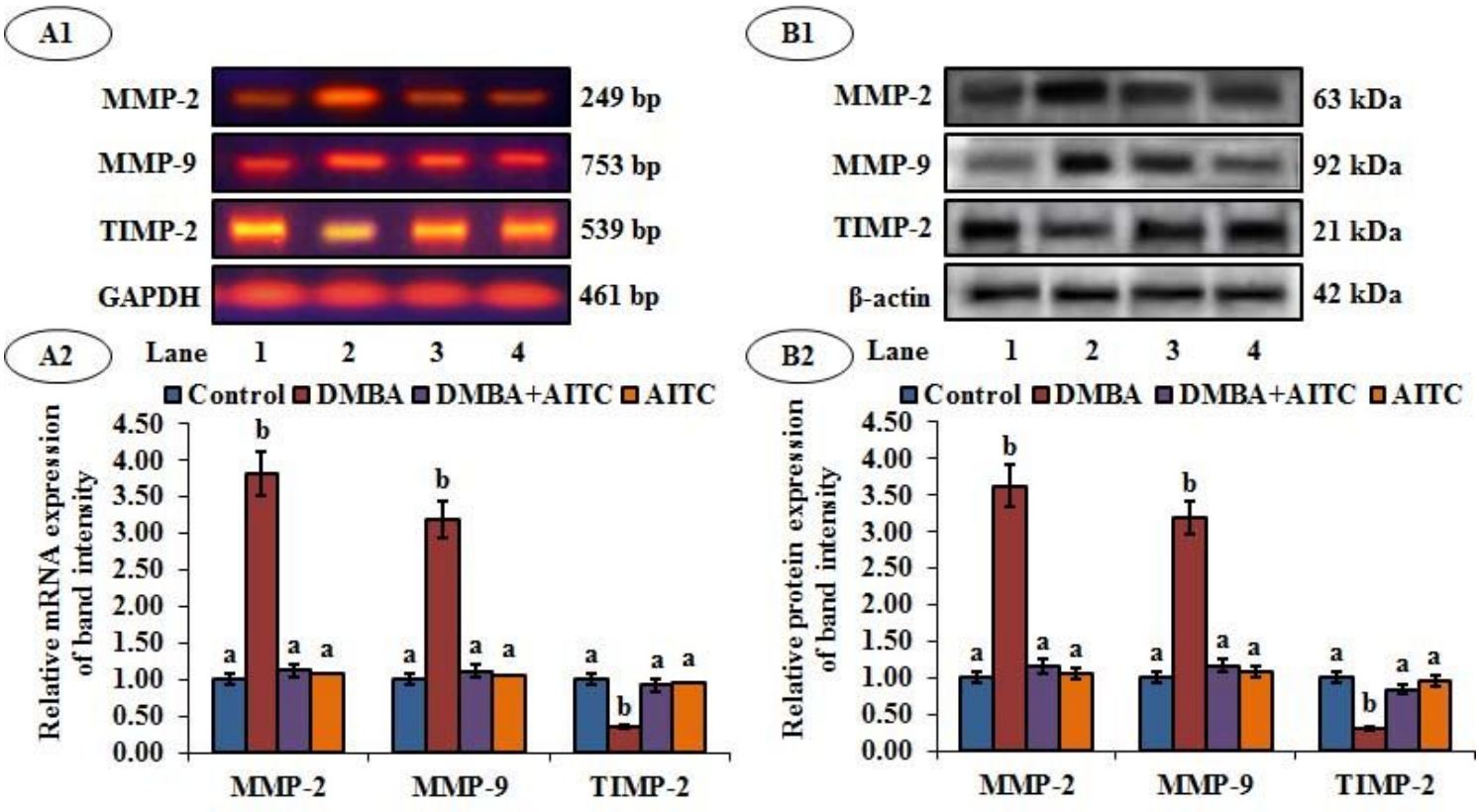

Figure 5

Expressions of MMP-2, MMP-9, and TIMP-2 in mammary tissues of control and experimental rats. (A1) Representative RT-PCR analysis shows the band intensity quantified by densitometry and normalized to respective GAPDH loading control. (A2) Representative graph shows the relative mRNA expression of fold changes in RT-PCR. (B1) Representative western blotting analysis shows the band intensity quantified by densitometry and normalized to respective β-actin loading control. (B2) Representative graph shows the relative protein expression of fold changes in western blot. Lane 1: control rats; Lane 2: DMBA injected rats; Lane 3: DMBA with AITC treatment; Lane 4: AITC only administered rats. Values are set as mean ± SD for 10 rats in each group. Values not sharing a common superscript differ substantially at $p<0.05$.

Fig. 6

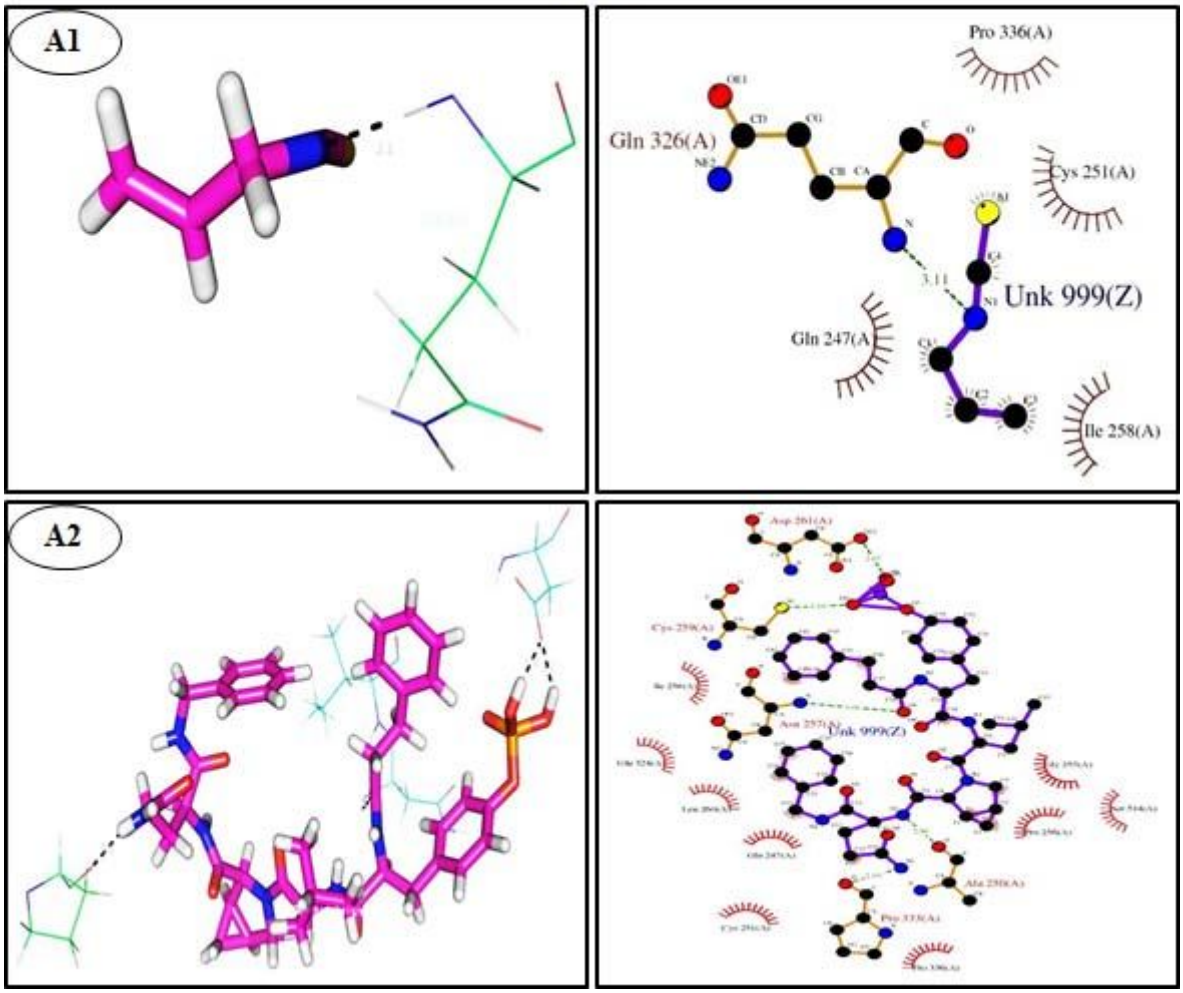

Figure 6

Representations of the binding mode of AITC with STAT-3 (A1) and the cocrystal structure of STAT-3 (A2).

Fig. 7

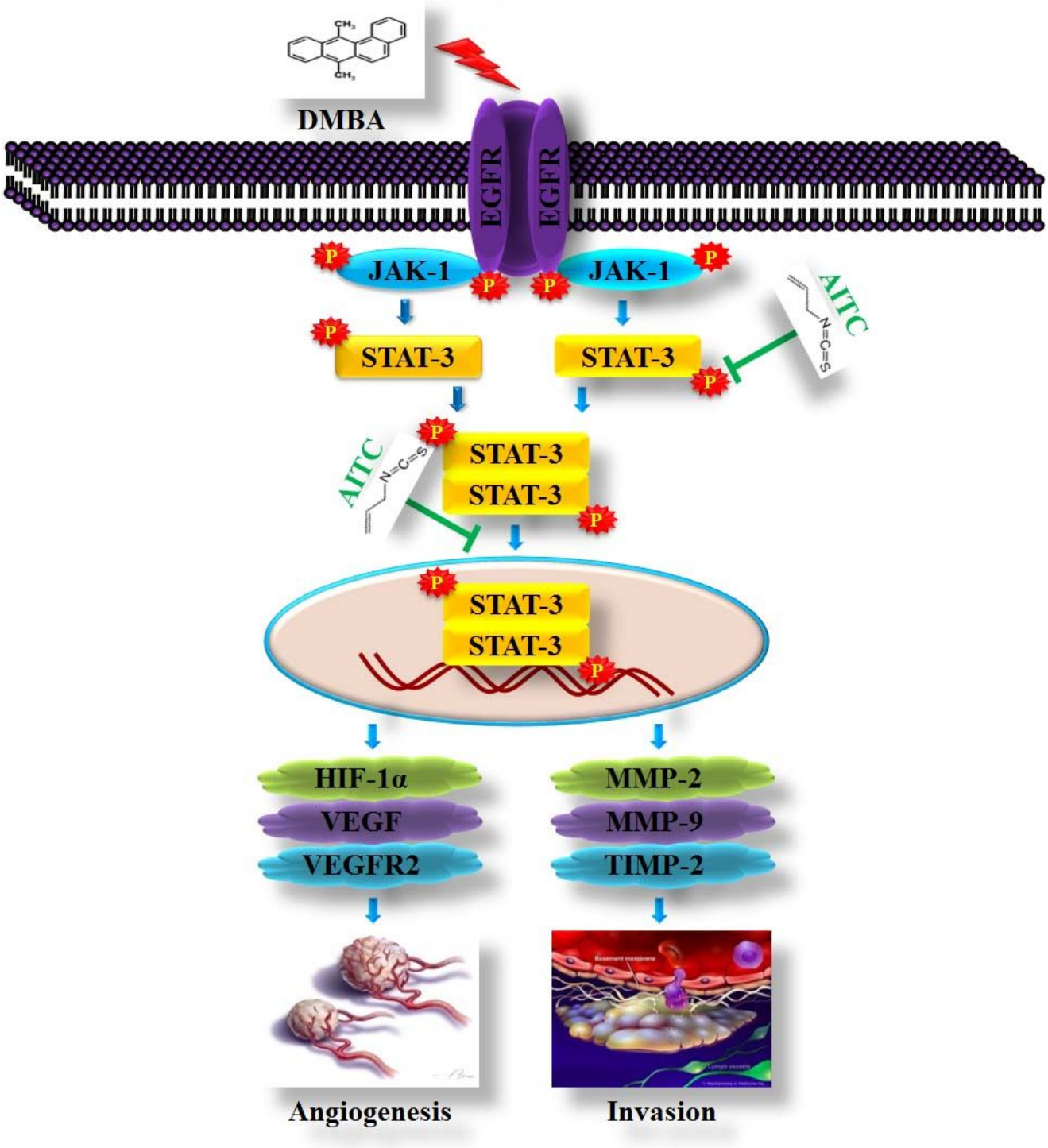

Figure 7

Schematic illustration of possible mechanisms of AITC during DMBA injected mammary tumorigenesis via a JAK-1/STAT-3 signaling pathway.